NASA TECHNICAL NOTE

NASA TN D-5234

c. 1

NASA TN D-5234

CALORIMETRIC EVALUATION OF THREE 1.5-METER-DIAMETER INFLATABLE RIGIDIZED SOLAR CONCENTRATORS

by Marvin D. Rhodes

Langley Research Center

Langley Station, Hampton, Va.

NATIONAL AERONAUTICS AND SPACE ADMINISTRATION • WASHINGTON, D. C. • JUNE 1969

CALORIMETRIC EVALUATION OF THREE 1.5-METER-DIAMETER INFLATABLE RIGIDIZED SOLAR CONCENTRATORS

By Marvin D. Rhodes

Langley Research Center
Langley Station, Hampton, Va.

NATIONAL AERONAUTICS AND SPACE ADMINISTRATION

For sale by the Clearinghouse for Federal Scientific and Technical Information
Springfield, Virginia 22151 – CFSTI price $3.00

CALORIMETRIC EVALUATION OF THREE 1.5-METER-DIAMETER INFLATABLE RIGIDIZED SOLAR CONCENTRATORS

By Marvin D. Rhodes
Langley Research Center

SUMMARY

The calorimetric efficiency of two 1.52-meter-diameter inflatable rigidized solar concentrators has been determined in order to evaluate their potential use with solar dynamic-cycle power systems. The membranes for these models were fabricated by different construction techniques and rigidized in a simulated space-vacuum environment with different foam materials (polyurethane and epoxy). Neither model was capable of satisfying typical design requirements of dynamic-cycle systems. The polyurethane-foam model had the higher calorimetric efficiency of the two models (0.61 at an aperture ratio of 7.6 as compared with 0.43 for the epoxy-syntactic-foam model); however, both models had about the same contour accuracy. In addition, these two models were compared with an epoxy—fiber-glass model rigidized at atmospheric pressure. Failure of all three models to meet the typical design requirements of the Brayton and Rankine cycle systems is due to low geometrical accuracy and low specular reflectance.

INTRODUCTION

Several methods have been investigated for converting solar energy into usable electrical power for space vehicles. One such solar dynamic-cycle system has the potential for supplying power loads up to 40 kilowatts and is being considered for long-term space missions (see ref. 1). The diameter of one-piece solar concentrators which have been considered for use with the dynamic conversion system (refs. 1 and 2) is limited by the diameter of the launch vehicle. Consequently, much effort has gone into the development of expandable concentrators such as the petalous (ref. 3), foldable Fresnel (ref. 4), and inflatable rigidized (ref. 5) types.

The inflatable rigidized concentrator is of particular interest because it can be folded into a compact package for launch (ref. 6). This concentrator would be formed in space by inflating and rigidizing an aluminized paraboloidal membrane. Several rigidizing materials have been formulated and used to rigidize solar concentrators in both a vacuum environment and at atmospheric pressure (refs. 7 to 11).

The purpose of this investigation was to determine the suitability of two inflatable rigidized solar concentrators, fabricated in a simulated space-vacuum environment, for use with dynamic-cycle power systems. This purpose was accomplished by measuring the calorimetric efficiencies of the two concentrators and comparing the efficiencies with typical design requirements of the Brayton and Rankine cycle systems (refs. 1 and 3). In addition, the calorimetric efficiencies of these models were compared with the efficiency of a model rigidized at atmospheric pressure. The latter concentrator was fabricated by a process not readily adaptable to space use and of materials known to give good geometric characteristics. All models were about 1.5 meters in diameter and each was rigidized with a different material.

The calorimetric efficiencies of the test models were determined by solar tracker tests. A water-cooled cavity calorimeter with aperture diameters ranging from 1.48 to 11.36 solar-image diameters was used as the heat receiver. The model rigidized at atmospheric pressure also received optical-ray-trace tests to determine concentrator-surface-slope errors. These errors were compared with the surface-error data reported in references 10 and 11 for the simulated-space-vacuum rigidized models.

SYMBOLS

The units used for physical quantities defined in this paper are given in the International System of Units (SI). Factors relating this system to U.S. Customary Units are presented in reference 12.

f_a distance along concentrator axis from concentrator vertex to calorimeter aperture, centimeters

f_d design focal length of concentrator model, centimeters

i,j,k orthogonal coordinate system (see fig. 13), with the origin on the surface of the design paraboloid, the k-axis along the paraboloid normal, and the j-axis intersecting the paraboloid axis

R_a radius of calorimeter aperture, centimeters

R_c measured radius of solar concentrator, centimeters

R_i radius of solar image formed in focal plane by cone of rays reflected from design paraboloid vertex, $f_d \tan \alpha$, centimeters

r	radial distance from concentrator axis measured along concentrator radius, centimeters
x	distance from concentrator axis to center of calorimeter aperture, measured along an axis normal to concentrator axis, centimeters
α	half-angle subtended by sun, 4.6 milliradians
δ_c	circumferential slope error of reflective surface, angle between the paraboloid normal and a projection of the concentrator normal on the ik-plane (fig. 13(b)), milliradians
δ_r	radial slope error of reflective surface, angle between the paraboloid normal and a projection of the concentrator normal on the jk-plane (fig. 13(b)), milliradians
η_c	calorimetric efficiency, ratio of energy absorbed by calorimeter water to energy incident on the concentrator
η_g	geometric efficiency, ratio of energy absorbed by calorimeter water to total energy specularly reflected from concentrator

MODELS

Fundamental Concept

An inflatable rigidized concentrator for space application would be formed by attaching an aluminized paraboloidal membrane to a section of a thin-plastic spherical membrane to form a balloon (see fig. 1). This balloon can be easily folded and packaged into a launch capsule; once in space, it would be deployed and inflated. The paraboloidal membrane would then be rigidized and the spherical plastic membrane discarded.

Two methods of rigidizing the paraboloid in space have been investigated and are reported in reference 13. In one method a foam generator is used which mixes the foam constituents and forces the foam over the concentrator rear surface. In the second method a precoat formulation is applied to the rear surface of the paraboloidal membrane before it is packaged for launch. Upon inflation the precoat would foam and rigidize as a result of exposure to some constituent of the space environment such as solar radiation.

Model 1

Model 1 was a paraboloid with a design rim angle of 1.05 radians and a diameter of 1.52 meters. A sketch and photograph of the model are shown in figure 2. The paraboloidal membrane was fabricated from a 25-micrometer-thick aluminized polyimide film. Twenty-four sectors were cut from the film and seamed together over a quasi-paraboloidal convex mold. The quasi-paraboloidal mold was designed to account for material strains that occur when the membrane is inflated. The membrane was then sealed to the periphery of a flat circular plate for inflation in a vacuum chamber. The circular plate replaced the spherical balloon as a pressure container in order to simplify the fabrication process. A layer of precoat formulation was then applied to the rear surface of the inflated membrane. This formulation was foamed in a simulated space-vacuum environment at a pressure of about 0.13 N/m^2 (1 newton per square meter = 0.0075 torr) by heating the precoat to 360° K. The process takes about 30 minutes from initiation of the foam to the end of cure. The resulting polyurethane foam was approximately 8 millimeters thick, and the aluminized film and rigidized foam had a ratio of mass to projected area of about 0.61 kg/m^2. A rim-support ring was bonded to the concentrator to provide sufficient stiffness for handling and testing. The rim-support ring, fabricated from an aluminum tube, was bonded to the back of the concentrator by encapsulation in a semi-flexible foam. A complete description of the model and fabrication details may be found in reference 10.

Model 2

Model 2 was a paraboloid with a design rim angle of 0.78 radian and a diameter of 1.52 meters. A sketch and photograph of the model are shown in figure 3. The membrane was fabricated from 51-micrometer-thick aluminized polyethylene-terephthalate film. The paraboloidal contour was formed by the stretch-relaxation process (ref. 11). This technique is used to form the paraboloidal contour by over-inflating a flat membrane to an oblate ellipsoid and then reducing the pressure until the desired paraboloid is formed. The precoat formulation is then applied to the pressurized membrane. Upon repressurization in space, the coated membrane will again form the desired paraboloidal contour. Film of sufficient width was not available to permit fabrication of model 2 from a single piece; therefore two pieces were seamed together by a reinforced butt joint. The membrane was sealed around a plate and inflated. An epoxy-syntactic precoat foam was spread on the convex side of the membrane. This precoat foam formulation consisted of small, hollow phenolic spheres in an epoxy-resin matrix. The precoat was backed by two perforated diaphragms which allowed excess gases to escape during heating. Curing was performed in a simulated space-vacuum environment at a pressure of 620 N/m^2 and a temperature of about 380° K for about 24 hours. The resulting foam was approximately

4 millimeters thick and the plastic film and foam had a mass-to-projected-area ratio of about 2.1 kg/m^2. A rim-support ring fabricated from a fiber-glass and epoxy tube was bonded to the rear surface of the shell in order to facilitate handling and testing. A complete description of the development and fabrication of this model is given in reference 11.

Model 3

Model 3 was a paraboloid with a design rim angle of 1.05 radians and a diameter of 1.52 meters. A sketch and photograph of the model are shown in figure 4. The paraboloidal membrane for this model was fabricated from 24 film sectors over the same mold and in the same manner as model 1. The membrane material was 25-micrometer-thick aluminized polyethylene terephalate. Upon inflation of the membrane, a coat of epoxy was applied and allowed to cure. Then three plies of fiber glass impregnated with epoxy resin were applied. The entire rigidizing process was performed at atmospheric pressure and room temperature. The shell thickness was about 0.8 millimeter and the concentrator shell had a mass-to-projected-area ratio of about 1.38 kg/m^2. The shell was reinforced at the perimeter by a rim-support ring of epoxy and fiber glass. The rim-support ring was bonded to the shell through a web in order to prevent reflective surface distortion in the contact region. A more detailed description of the model may be found in reference 13.

APPARATUS AND TEST PROCEDURE

Calorimetric Tests

The solar tracker used for the calorimetric tests was a converted searchlight that has been instrumented to track the sun automatically in both azimuth and elevation with an accuracy of ±0.1 milliradian. A photograph of the tracker with model 3 is shown in figure 4(b). The calorimeter which was placed in the focal region during tests consisted of a blackened copper helical coil surrounded by insulation and encased in a stainless-steel cylinder. The calorimeter was equipped with a set of aperture plates with different size orifices. A 25-centimeter-diameter water-cooled face plate was placed in front of the aperture plate to carry off the energy falling on the aperture plate and calorimeter case. A more detailed description of the apparatus and test procedure is given in reference 14.

All three concentrators were tested to determine the effect, on calorimetric efficiency, of aperture size and aperture location in the focal region. Test variables included aperture sizes from $1.48R_i$ (1.27 centimeters in diameter) to $11.36R_i$ (6.98 centimeters in diameter), axial locations of calorimeter aperture from $0.99f_d$ to $1.05f_d$, and lateral movement of the calorimeter aperture of $\pm 1.8R_i$.

Additional tests were made on model 3 to evaluate the effects on efficiency of areas near the seams and near the rim where visual observation indicated reflective-surface defects were present. In order to evaluate the seam area, a radial mask was constructed to intercept the solar radiation falling on the seams. The projected seam area covered by the mask was about 17 percent of the usable projected area of the concentrator. A photograph of this mask on the solar tracker is shown in figure 5(a). An annular mask was constructed to evaluate the concentrator rim region where an orange-peel effect was noted. The area obscured by this mask was about 25 percent of the usable projected area of the concentrator. A photograph of this mask on the solar tracker is shown in figure 5(b).

The calorimetric efficiencies greater than about 0.40 are considered accurate to within ±0.02 on the basis of instrument component errors and repeatability of data. Efficiencies less than about 0.40 have larger errors (±0.03) because the calorimeter flow meter and temperature sensing system were used in a less accurate region of their operating range.

Optical-Ray-Trace Tests

The optical-ray-trace fixture shown in figure 6 was used to perform surface-slope-error tests on model 3. A beam of collimated light about 5 millimeters in diameter, directed parallel to the concentrator axis, was reflected to a focal-plane-image plate. The displacements of the collimator images from the concentrator axis were recorded. The concentrator surface was surveyed near the center of each sector along 5 radial stations. Additional data were taken across two seams at two radial stations in order to evaluate the seam area. These data were used to calculate a system of error angles for the concentrator surface. A complete description of the test apparatus and procedure is given in reference 15.

Errors in measuring the displacement of the focal-plane image from the concentrator axis produced inaccuracies in the reflective-surface error angles. This uncertainty in slope-error angles depends upon the test radial distance r and varies from 0.38 milliradian for δ_c and 0.35 milliradian for δ_r at the inner test radius (that is, at $r = 0.217R_c$) to 0.34 milliradian for δ_c and 0.17 milliradian for δ_r at the outer test radius (that is, at $r = 0.867R_c$).

Spectrophotometric Tests

Spectrophotometric tests were made on samples cut from concentrators similar to test models 1 and 2 in order to determine the solar specular reflectance of these models. Since no samples of the model 3 laminate were available, tests were run on unreinforced

samples of aluminized polyethylene terephalate. These tests were made over a wavelength range of 300 to 1800 nanometers with a spectrophotometer having an integrating-sphere attachment. The specular reflectance of the samples was determined indirectly by separately measuring the specular plus diffuse reflectance and the diffuse reflectance. The measured values of reflectance are relative to a standard which must be used with the integrating-sphere attachment. The absolute reflectance values of the standard are then used to convert the measured reflectance values to absolute values. The specular-reflectance standard was an aluminized front-surface mirror with no overcoating, and the diffuse-reflectance standard was a block of magnesium carbonate with a new surface exposed. The absolute values of spectral specular reflectance were converted to values of solar specular reflectance by applying spectral solar irradiance over the wavelength range of 300 to 1800 nanometers.

Flat samples similar to the concentrator laminates were not available for measurement during this investigation. Therefore, measurements were made on curved samples of concentrator surfaces, and independent tests were made to determine the effect of this curvature on the measured reflectance. A lens with about the same curvature as the test samples and a piece of plate glass were aluminized simultaneously in a coating apparatus. Spectrophotometric measurements on these two surfaces indicated that the difference in measured reflectance was within the accuracy of the data; therefore the curvature was considered to have no effect.

The accuracy of the specular reflectance obtained during this investigation is considered to be within ± 0.015 on the basis of data repeatability and known reflectance of the standards.

RESULTS AND DISCUSSION

A thorough search of the focal region was made for each model by varying the location of the calorimeter to determine the position of maximum efficiency. The axes surveyed were the concentrator axis and two orthogonal lateral axes. The test results for each model are presented and a comparative analysis of all models is made.

Model 1

The variation in calorimetric efficiency η_c with axial location of the calorimeter aperture f_a/f_d for the polyurethane-foam model is shown in figure 7. The distance of the calorimeter aperture from the concentrator vertex measured along the concentrator axis was nondimensionalized by the design focal length $f_d = 66$ centimeters. The concentrator focal length is considered to be the distance f_a where maximum efficiency occurs.

The focal length for this model is about $1.038f_d$ which is considerably longer (2.5 centimeters) than the design value of 66 centimeters. An analysis of the data in reference 10 also indicates that the focal length of this concentrator is longer than the design value and thus confirms the results in the present investigation. The extended focal length may be due to overpressurization of the membrane caused by the exotherm of the precoat as foaming is initiated. It should also be noted in figure 7 that the calorimetric efficiency is relatively insensitive to small changes in axial aperture location for every test aperture. This fact indicates that the concentrator has a large energy distribution. Consequently, the axial position of the heat receiver used with this model on a space-power system would not be too critical.

The variation in calorimetric efficiency with lateral location of the calorimeter aperture (x/R_i) for the polyurethane-foam model is shown in figure 8. For the test range of x/R_i very little change in calorimetric efficiency was noted, a factor which is also due to the large energy distribution in the focal plane.

Model 2

Calorimetric tests on the epoxy-foam model were made immediately after fabrication and are reported in reference 11. Data from reference 11 were checked by tests on the solar tracker in the present investigation. Lateral and axial calorimetric searches were made in the concentrator focal region; however, only the maximum values of efficiency were recorded. Results from reference 11 and from the present investigation are shown in figure 9. The considerable difference between the two sets of data may be attributed to several factors. The fact that the data were taken on two different solar trackers with different calorimeters could account for some of the difference. The tests reported in reference 11 were made immediately after fabrication, whereas the present investigation was conducted several weeks later. The rim-support ring was relatively light and may have allowed the concentrator to distort during shipping and storage.

Model 3

The variation in calorimetric efficiency with axial location of the calorimeter aperture for the epoxy—fiber-glass model is shown in figure 10. For this model also, f_a was nondimensionalized by the 66-centimeter design focal length f_d. It can be seen from the figure that the maximum efficiency for the different apertures does not occur at the same axial aperture location. This fact indicates that the surface is a quasi-paraboloid. For all test-aperture sizes, maximum efficiency occurs at a location f_a/f_d greater than 1.00. For the largest aperture ratio the focal length is about 66.2 centimeters ($f_a = 1.003f_d$), and for the smallest aperture ratio the focal length is about 67.4 centimeters ($f_a = 1.021f_d$). It should also be noted that even though this concentrator

does not have a single focal point, all focal lengths are closer to the design focal length than the focal length for the polyurethane-foam model (model 1). This fact is probably due to the fabrication process and materials, since the membranes for both models were made over the same die. The data shown in figure 10 also indicate that the performance of the concentrator is relatively insensitive to axial aperture location, as was noted for the polyurethane-foam model.

The variation in concentrator efficiency with lateral location of the calorimeter aperture for the epoxy—fiber-glass model is shown in figure 11. These data were taken with the calorimeter positioned at the optimum axial location for each test aperture, as shown in figure 10. The performance of the concentrator is relatively insensitive to the lateral position (x/R_i) of the calorimeter aperture, and the maximum value for all apertures occurs at or near the zero position. Data taken along the other lateral axis were similar to the data shown; therefore the energy distribution was assumed to be symmetrical about the concentrator axis.

Visual inspection of the model indicated that several areas appeared to be less accurate than the majority of the concentrator surface. Therefore, tests were made with masks which obscured the seam area and an annulus at the periphery. The variations in calorimetric efficiency with aperture ratio for both the masked and unmasked concentrator are shown in figure 12. The test data for the unmasked condition are the maximum values from the searches shown in figures 10 and 11. The data for the two masked conditions were obtained from searches of the focal region similar to those for the unmasked condition and, therefore, do not necessarily represent the same position of the calorimeter. Data from both of the masked-concentrator tests show an improvement over the unmasked-concentrator results at all aperture ratios.

Two conditions may exist which are responsible for this improved performance. The masks could be blocking areas with poor geometry, or the blocked areas could have a lower specular reflectance than the integrated specular reflectance of the total concentrator. These effects are difficult to separate, since there are no available samples of model 3 on which reflectance measurements could be made. Visual inspection of the concentrator surface indicated an orange-peel effect near the rim. This observation was substantiated by optical-ray-trace tests in which the collimated light reflected to the focal-plane-image plate was diffused and in some instances could not be seen. However, it could not be determined if this diffusion was due to a loss in specular reflectance or small geometric imperfections.

The effects of reflectance and geometry on concentrator performance are also difficult to separate when the seams are masked (see fig. 12). Visual inspection of the seams did not indicate the presence of the orange-peel effects noted previously at the rim. However, a measure of the relative geometrical accuracy of the seams can be

determined from the circumferential surface-slope error δ_c. This angle, which is shown in figure 13, was calculated from optical-ray-trace data taken across the sectors and seams. The circumferential error as a function of the angular displacement from the sector center line is shown in figure 14. These data represent two radial stations across two randomly selected sectors. The errors are largest and change very rapidly in the vicinity of the seams. Therefore, the increase in calorimetric efficiency for the seams-masked data as compared with the unmasked data (fig. 12) is apparently due to masking large surface-slope errors near the seams.

Comparison of All Models

The efficiency of all models as a function of aperture ratio is shown in figure 15(a). All data were obtained during the present investigation and represent peak values from the focal-region surveys. Also shown in the figure are two concentrator design points (from refs. 1 and 3) for dynamic-cycle systems. None of the test models met the typical design specifications for either the Brayton or the Rankine cycle systems. Therefore, for a given power level these concentrators must have a larger diameter than those with the design specifications considered in references 1 and 3. It should be noted that the epoxy—fiber-glass model (model 3) had the highest calorimetric efficiency of the three models at every aperture ratio. At the aperture ratio considered for the Rankine cycle system (7.6), this model had an efficiency of 0.66 as compared with 0.61 and 0.43 for the polyurethane-foam model (model 1) and the epoxy-syntactic-foam model (model 2), respectively.

Failure of all models to meet the design specifications for the dynamic-cycle systems may be due to either low geometric efficiency or poor specular reflectance. Values of specular reflectance for models 1 and 2 were determined from spectrophotometric measurements made on samples cut from concentrators similar to the test models. The solar specular reflectance was 0.85 for model 1 and 0.82 for model 2. As mentioned previously, no direct reflectance measurements were made on samples of model 3; however, the reflectance of this model would not be expected to be higher than that of the unreinforced aluminized membrane. The reflectance of the membrane material measured in the present investigation was about 0.85, which agrees well with reported measurements of about 0.83 from other investigations (refs. 10 and 16). Therefore, it may be assumed that the specular reflectance of model 3 did not exceed an average value of about 0.84. It should also be noted that the values of reflectance measured on the samples cut from concentrators similar to models 1 and 2 are about the same as the reflectance measured on the unreinforced membrane materials. Therefore the application of the rigidizing foams has not significantly lowered the reflectance of the membranes used for these concentrators. The reflectance values for all the concentrators are somewhat

below the dynamic-cycle design values of about 0.91 that were used in references 1 and 3. Since the maximum efficiency obtainable is the specular reflectance of the concentrator surface, the failure of these models to meet the typical dynamic-cycle design specifications is partially due to low specular reflectance.

The variation in geometric efficiency with aperture ratio is shown in figure 15(b). The geometric efficiencies for models 1 and 2 were obtained by dividing the calorimetric efficiency from figure 15(a) by the specular reflectance of each model. The data for model 3 were obtained by dividing the calorimetric efficiency with the perimeter masked (see fig. 12) by the average specular reflectance measured on aluminized-membrane materials (0.84). The perimeter-masked data were used for this comparison because it could not be determined if the low calorimetric efficiency at the rim was due to a loss in specular reflectance or small geometric imperfections. Also, the radial slope errors δ_r, which are discussed subsequently, could not be obtained near the concentrator rim and therefore represent the same area as the perimeter-masked data. None of the test models has the necessary geometric accuracy to satisfy the dynamic-cycle system requirements. Model 3 had the highest calorimetric efficiency, which is still about 0.11 below the design requirement of the Rankine cycle system, which has the lower geometrical-accuracy requirement of the two systems considered. There are two conditions present that can affect the concentrator geometric efficiency shown in figure 15(b). The concentrator may have small random geometric imperfections which cause a large energy distribution in the focal plane or the concentrator may not have the proper surface contour.

An indication of the relative contour accuracy of the concentrator models is given by the cumulative distribution of radial slope error δ_r for each model as shown in figure 16. Data for model 3 were obtained from optical-ray-trace tests made during this investigation and do not include the rim area because of the diffused image of the collimated light from this region. Data for the other models were obtained from references 10 and 11 and have been converted to radial slope error. Model 3, which had the highest geometric efficiency, also has a more accurate surface contour than the other models. The superior accuracy of this model may be attributed to construction from materials known to give good geometrical accuracy. Also, the model was rigidized at atmospheric pressure and room temperature instead of in a space-vacuum environment.

The similarity of the radial-slope-error distributions for models 1 and 2 is significant because these two models had large differences in geometric efficiencies. The low geometric efficiency of model 2 (see fig. 15(b)) is apparently due to localized geometric imperfections which are not detectable when using the surface-slope measuring techniques reported in reference 11. These imperfections can be seen in the photograph of model 2

shown in figure 3(b). The similarity in contour accuracy of these models is also significant because the models represent different membrane construction techniques. Each membrane construction technique has inherent problems which should be considered before selecting a method to construct a larger space model. A membrane of uniform thickness is desirable for the stretch-relaxation technique. Since sheet material is supplied in limited widths, large concentrators will require several sheets seamed together. The effect of these seams on the membrane contour should be evaluated before large models are constructed. The seams also present a problem for the sector-type membrane construction. The reinforcement of the seams does not permit the pressurized membrane to deflect uniformly, and a parachuting effect in the concentrator surface results. This effect can be observed in the data of figure 14 and is indicated by the increase in circumferential slope error across the sector.

It is interesting to note that model 1 does not have the contour accuracy or geometric efficiency of model 3 even though both models were fabricated from sectors over the same mold. The lower geometrical accuracy of model 1 (see figs. 15(b) and 16) is attributed to the foam material. The precoat used on this model foamed in small areas and propagated in "fronts" until the entire surface was rigidized. This process resulted in a wave effect in the reflective surface. Also, as noted previously, the precoat material gives off heat during the foaming operation which causes a pressure rise in the inflated membrane. This pressure fluctuation makes the surface contour difficult to control during rigidization.

CONCLUDING REMARKS

Results from two inflatable solar concentrators which were rigidized in a simulated space-vacuum environment have been evaluated and compared with typical design requirements for dynamic-cycle power systems. Neither model attained the design requirements; therefore for a given power level, these concentrators must have a larger diameter than those that do meet the design specifications. Failure of these models to meet the dynamic-system design specifications is due to low geometrical accuracy and low specular reflectance. The measured specular reflectance of the two models (0.85 for the polyurethane-foam model and 0.82 for the epoxy-syntactic-foam model) was somewhat below the dynamic-cycle design value of about 0.91. Both models had about the same contour accuracy even though they were fabricated by different membrane-construction techniques and with different rigidizing foams. The low geometric efficiency of the epoxy-syntactic-foam model is due to localized geometric imperfections.

The efficiencies of these two models were compared with the efficiency of an epoxy—fiber-glass model rigidized at atmospheric pressure and room temperature. Of the three

models tested, this model had the highest calorimetric efficiency (0.66 at an aperture ratio of 7.6 as compared with 0.61 for the polyurethane-foam model and 0.43 for the epoxy-syntactic-foam model). However, it also did not meet the design requirements of either the Brayton or the Rankine cycle system. The higher efficiency of this model was attributed to construction from materials and by techniques known to give good geometrical accuracy.

Langley Research Center,
National Aeronautics and Space Administration,
Langley Station, Hampton, Va., March 17, 1969,
120-33-06-11-23.

REFERENCES

1. Stewart, D. E.: Brayton Cycle Solar Collector Design Study. NASA CR-195, 1965.
2. Kovalcik, Edward S.; et al.: Brayton Cycle Solar Collector Design Study. NASA CR-54118, 1964.
3. Anon.: Sunflower Solar Collector. NASA CR-46, 1964.
4. Anon.: Experimental Reflector Orbital Shot (EROS). ASD-TDR-63-266, Vol. I, Pt. I, U.S. Air Force, Apr. 1963.
5. Lyman, Robert; and Houmard, James E.: Inflatable Foam-Rigidized Approach to Solar Concentrators. Power Systems for Space Flight, Morris A. Zipkin and Russell N. Edwards, eds., Academic Press, 1963, pp. 687-711.
6. Houck, O. K.; and Heath, A. R., Jr.: Characteristics of Solar Concentrators as Applied to Space Power Systems. Paper 867C, Soc. Automot. Eng., Apr. 1964.
7. Anon.: Investigation of a 15-kW Solar Dynamic Power System for Space Application. AFAPL-TR-64-156, U.S. Air Force, Feb. 28, 1965.
8. Hanny, J. F.; Jones, J. W.; Lankston, L. R.; and Scott, J. C.: Chemical Rigidization of Expandable Structures. AFAPL-TR-66-53, U.S. Air Force, Sept. 1966.
9. Jouriles, N.; and Welling, C. E.: Development of a Predistributed Azide Base Polyurethane Foam for Rigidization of Solar Concentrators in Space. NASA CR-235, 1965.
10. Jouriles, N.; Welling, C. E.; and Kryah, J. C.: Rigidization of a 1.52-Meter Diameter Inflatable Solar Concentrator in Vacuum With Associated Material Studies and Fabrication Techniques. NASA CR-66114, 1966.
11. Schwartz, S.; and Bagby, J.: Rigidized Inflatable Solar Energy Concentrators. NASA CR-254, 1965.
12. Comm. on Metric Pract.: ASTM Metric Practice Guide. NBS Handbook 102, U.S. Dep. Com., Mar. 10, 1967.
13. McCusker, Thomas J.: Solar Concentrator Design and Construction. Space Power Systems Engineering, George C. Szego and J. Edward Taylor, eds., Academic Press, 1966, pp. 687-700.
14. Willis, Conrad M.: Calorimetric Evaluation of a 60-Inch (152-Centimeter) Electroformed Nickel Solar Concentrator. NASA TN D-3012, 1965.

15. Willis, Conrad M.; and Houck, O. Karl: Geometric Efficiency of an Electroformed Nickel Solar Concentrator. NASA TN D-4072, 1967.

16. Nowlin, William D.; and Benson, Harold E.: Study of Umbrella-Type Erectable Paraboloidal Solar Concentrators for Generation of Spacecraft Auxiliary Power. NASA TN D-1368, 1962.

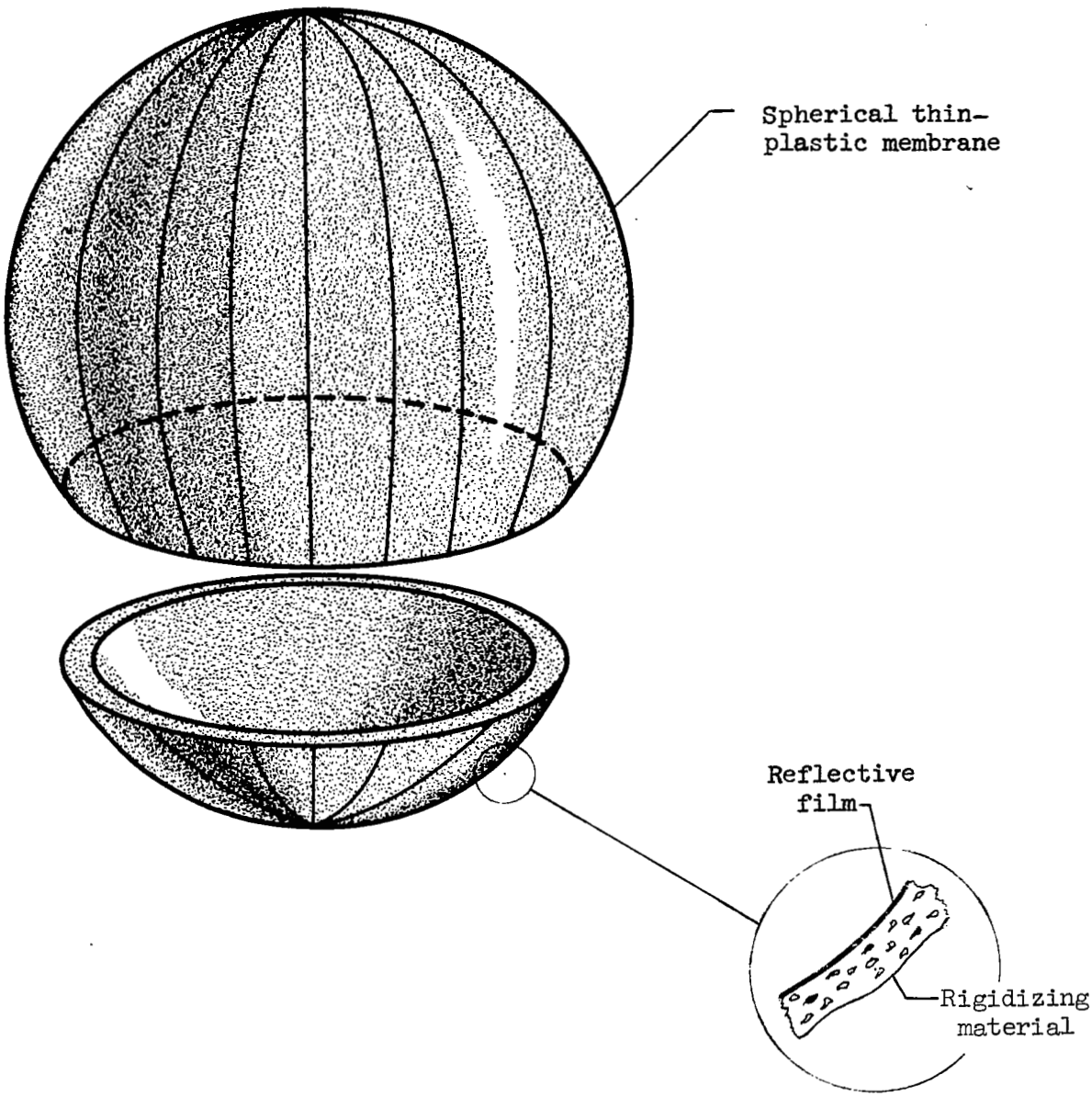

Figure 1.- Concept of inflatable rigidized solar concentrator.

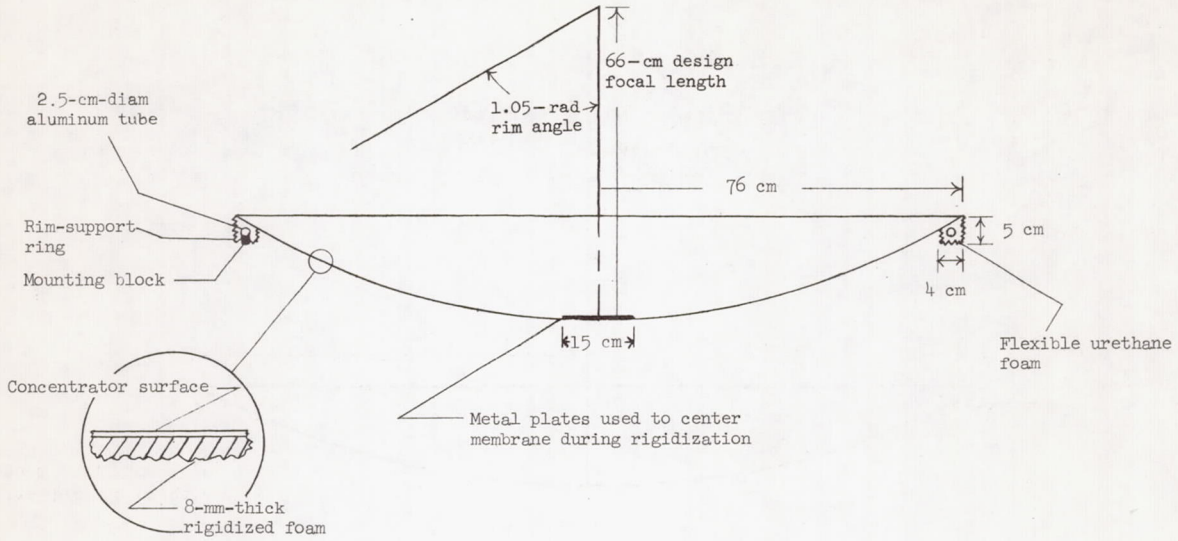

(a) Cross section of model 1 along a diameter showing design dimensions.

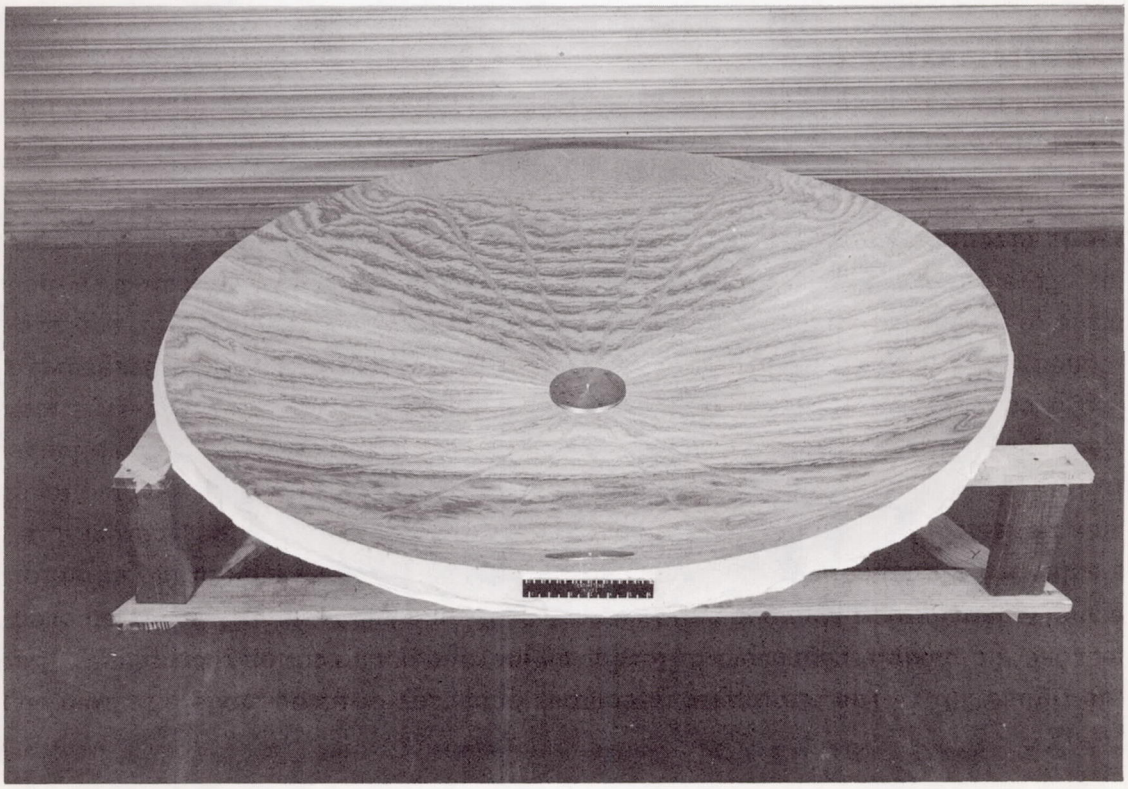

(b) Photograph of model. L-66-2968

Figure 2.- Model 1.

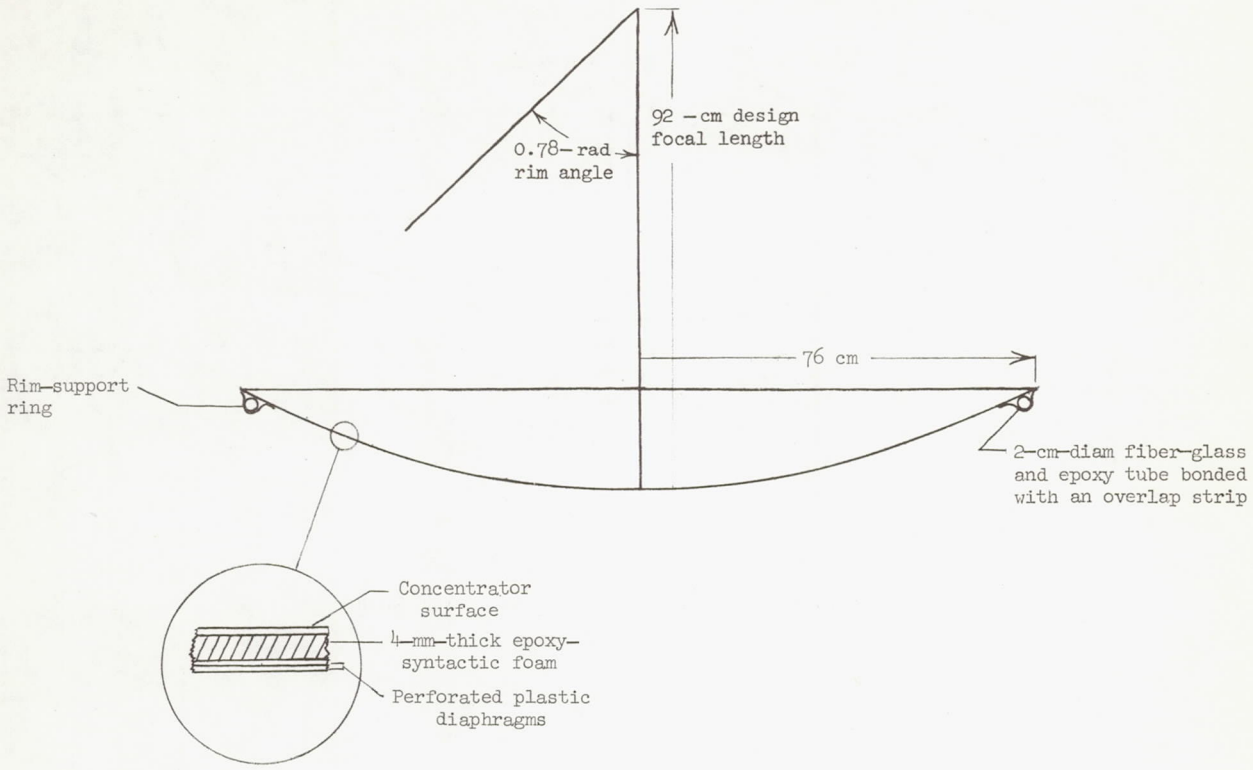

(a) Cross section of model 2 along a diameter showing design dimensions.

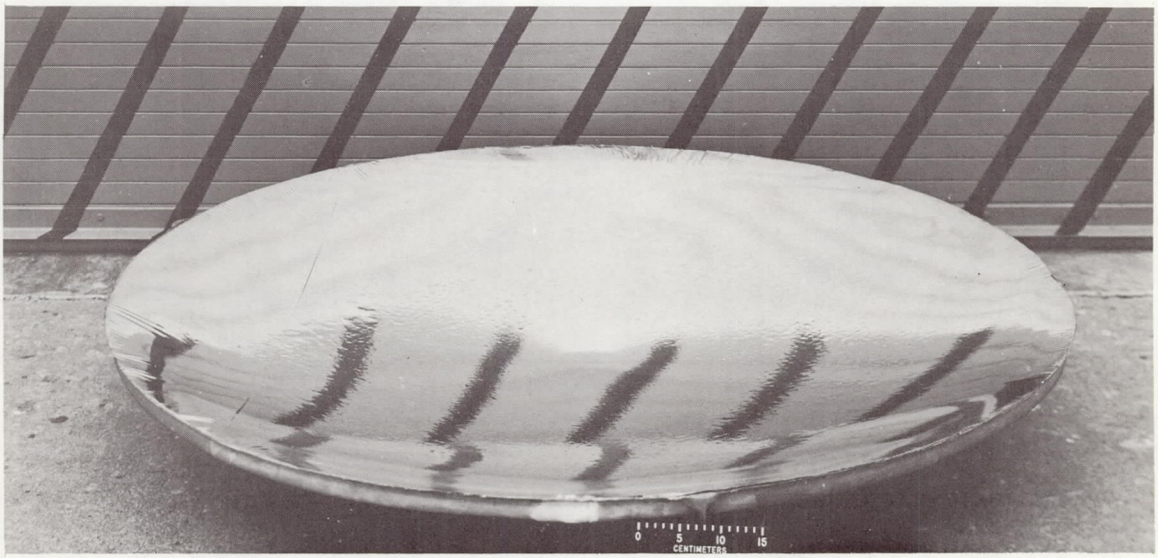

(b) Photograph of model. L-67-1226

Figure 3.- Model 2.

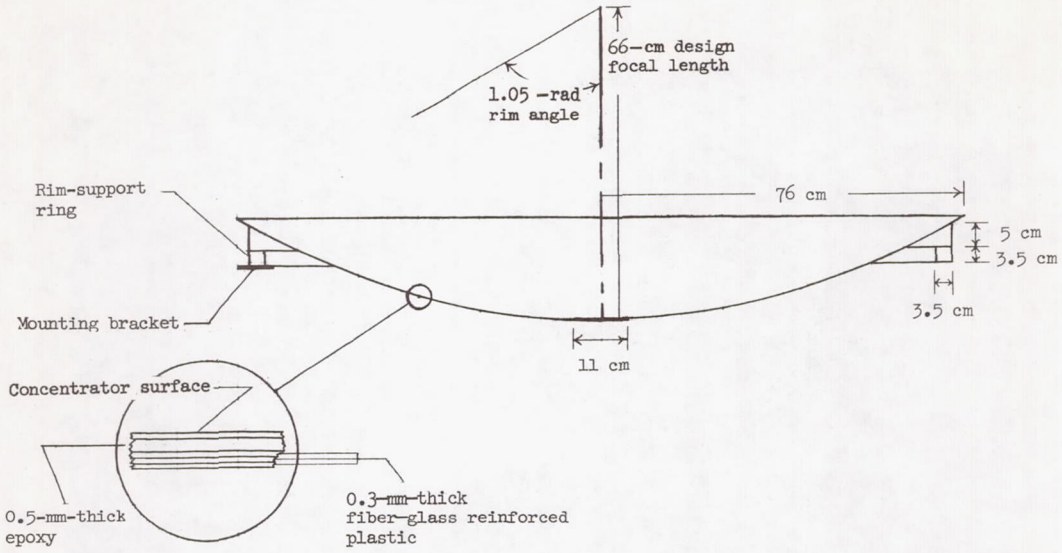

(a) Cross section of model 3 along a diameter showing design dimensions.

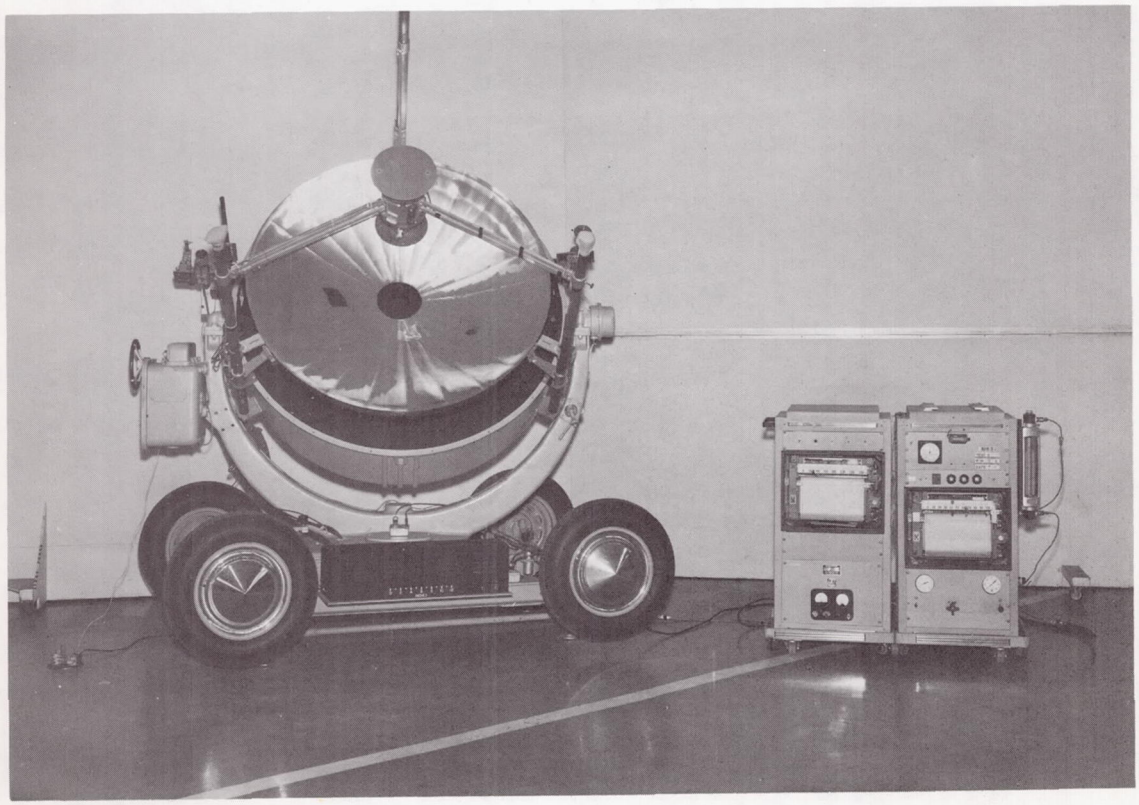

(b) Photograph of model in solar tracker. L-64-10854

Figure 4.- Model 3.

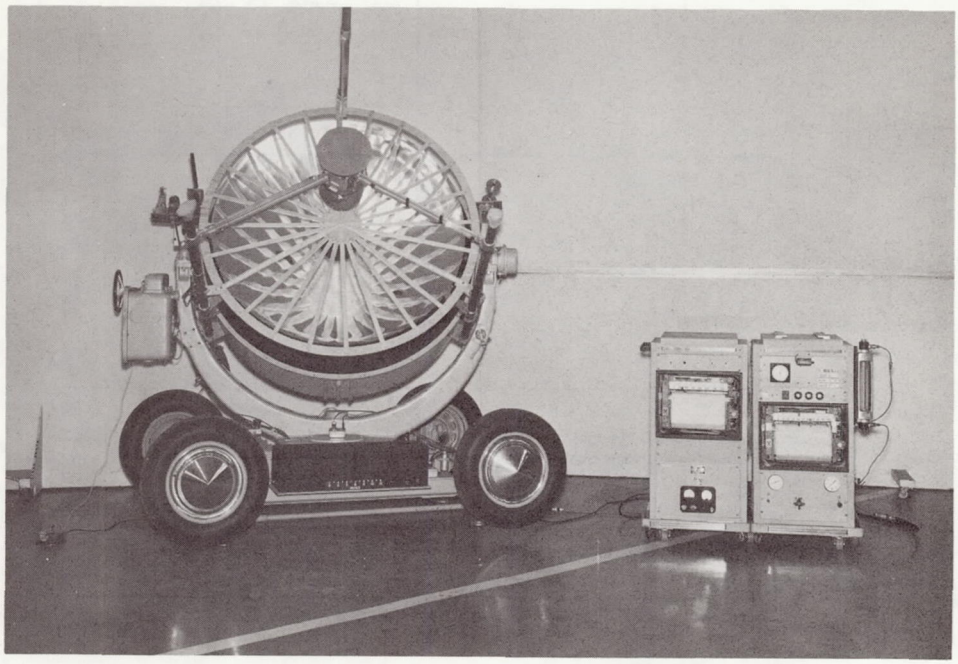

(a) Model 3 with seams masked. L-64-10856

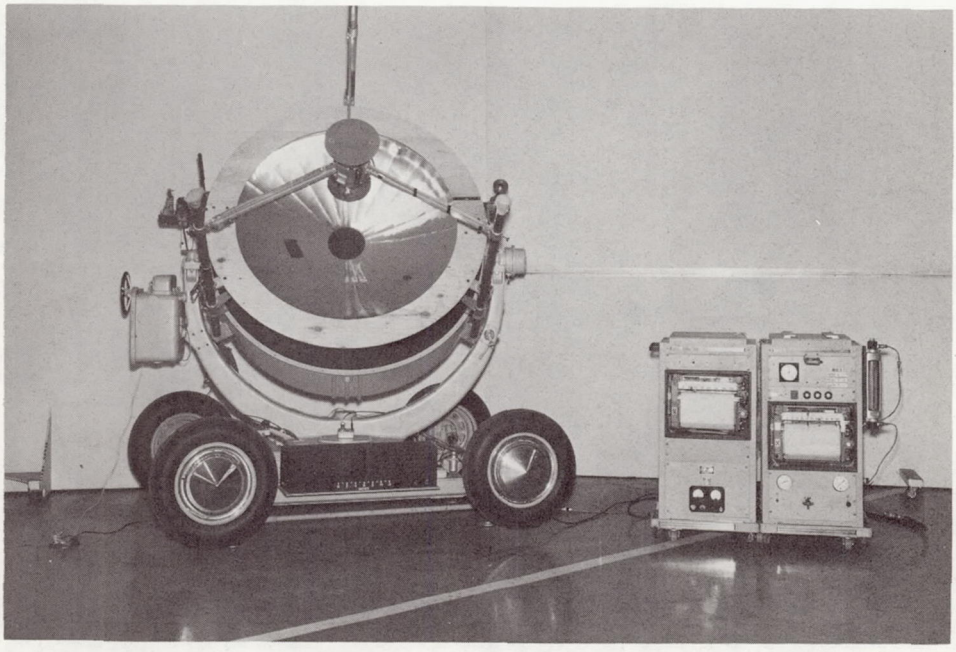

(b) Model 3 with perimeter masked. L-64-10855

Figure 5.- Photographs showing masks used to evaluate model 3.

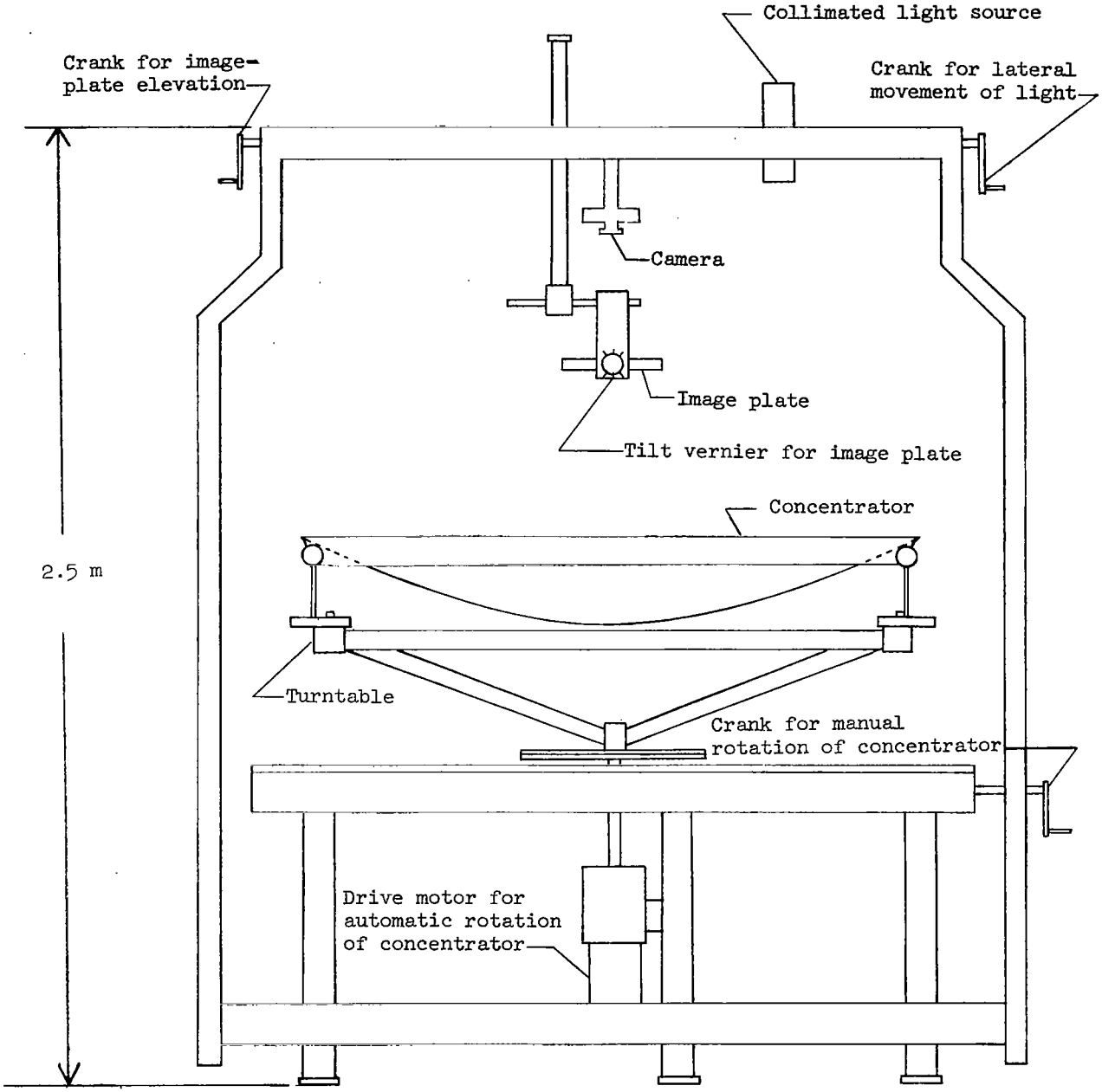

Figure 6.- Sketch of ray-trace test fixture.

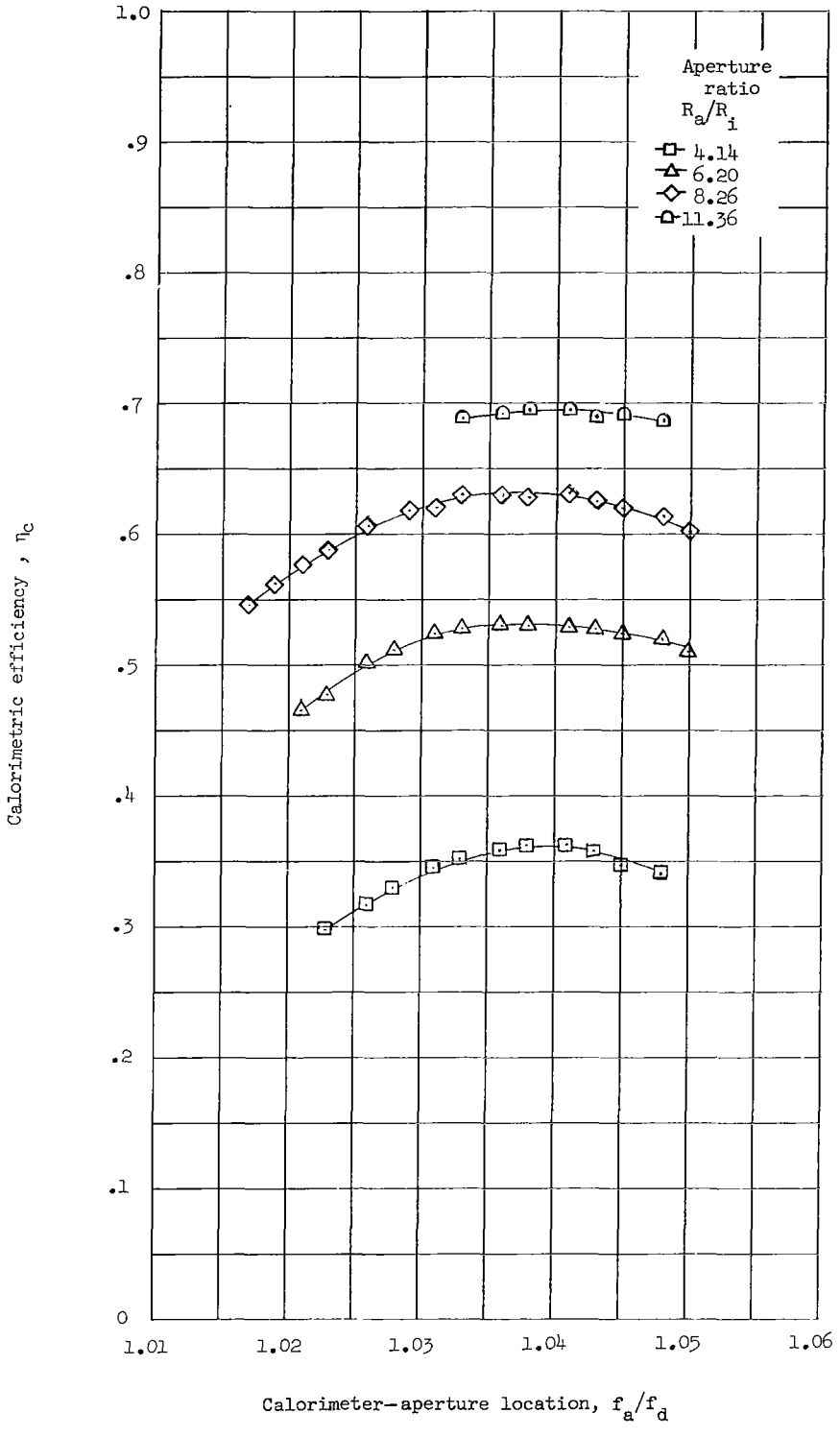

Figure 7.- Variation in calorimetric efficiency with axial location of calorimeter aperture for model 1.

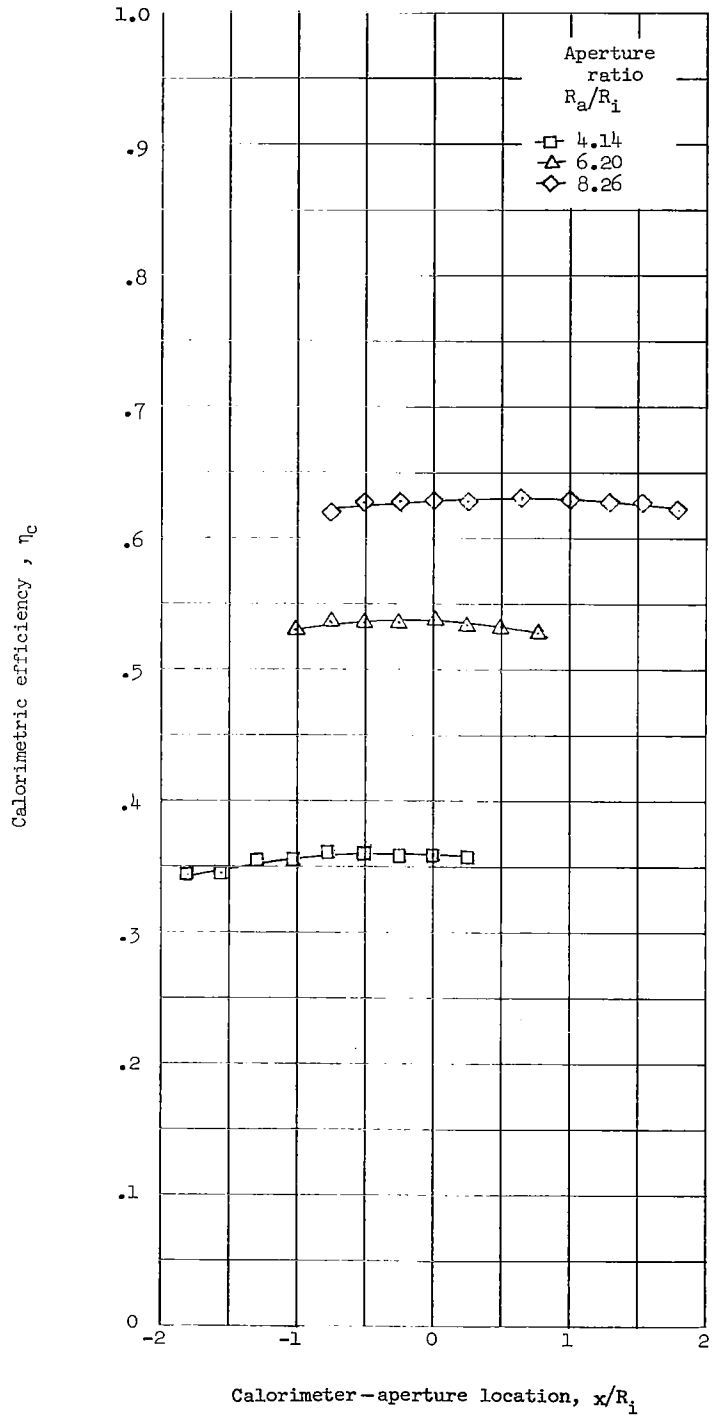

Figure 8.- Variation in calorimetric efficiency with lateral location of calorimeter aperture for model 1. $\frac{f_a}{f_d} = 1.038$.

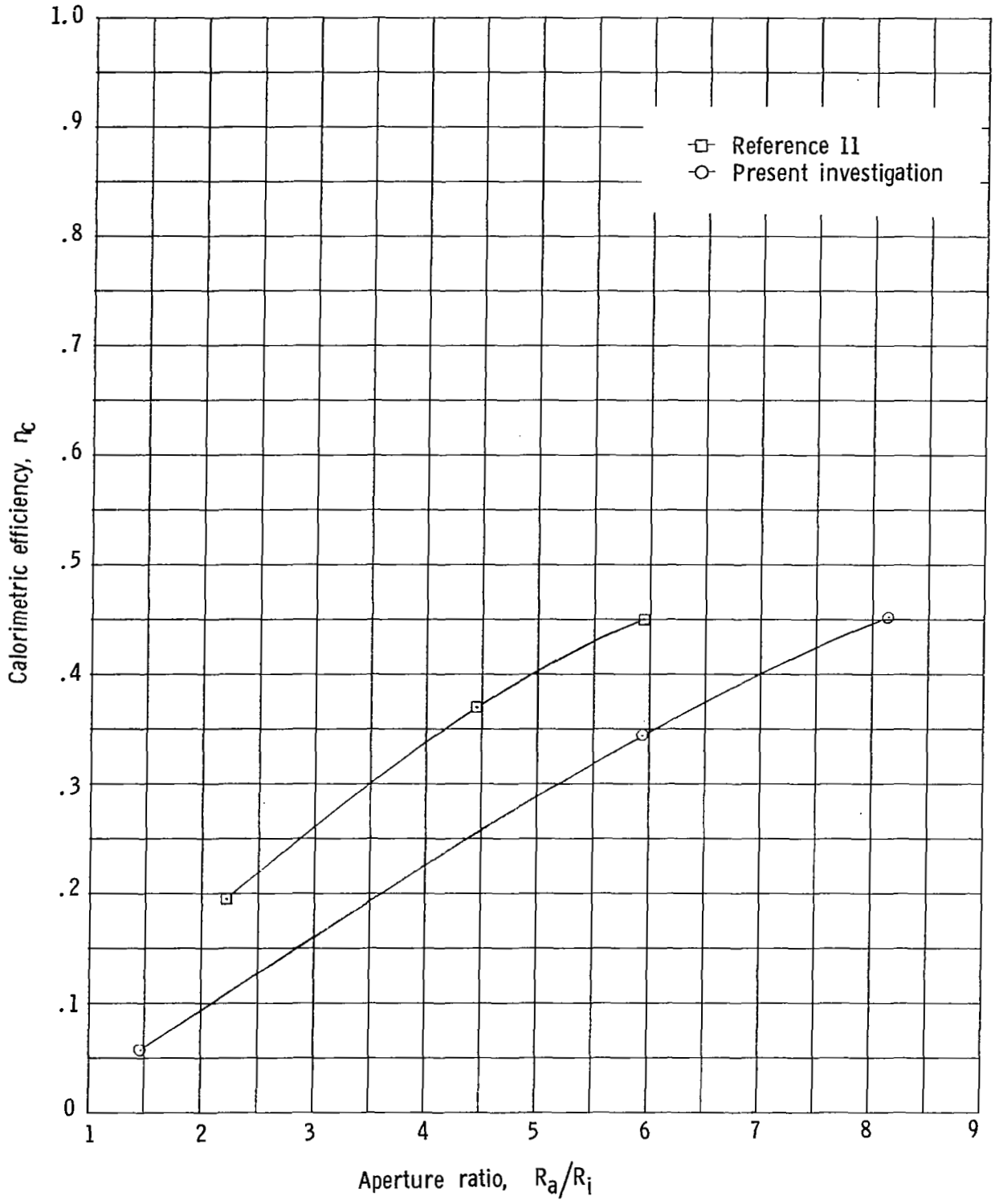

Figure 9.- Variation in calorimetric efficiency with aperture ratio for model 2.

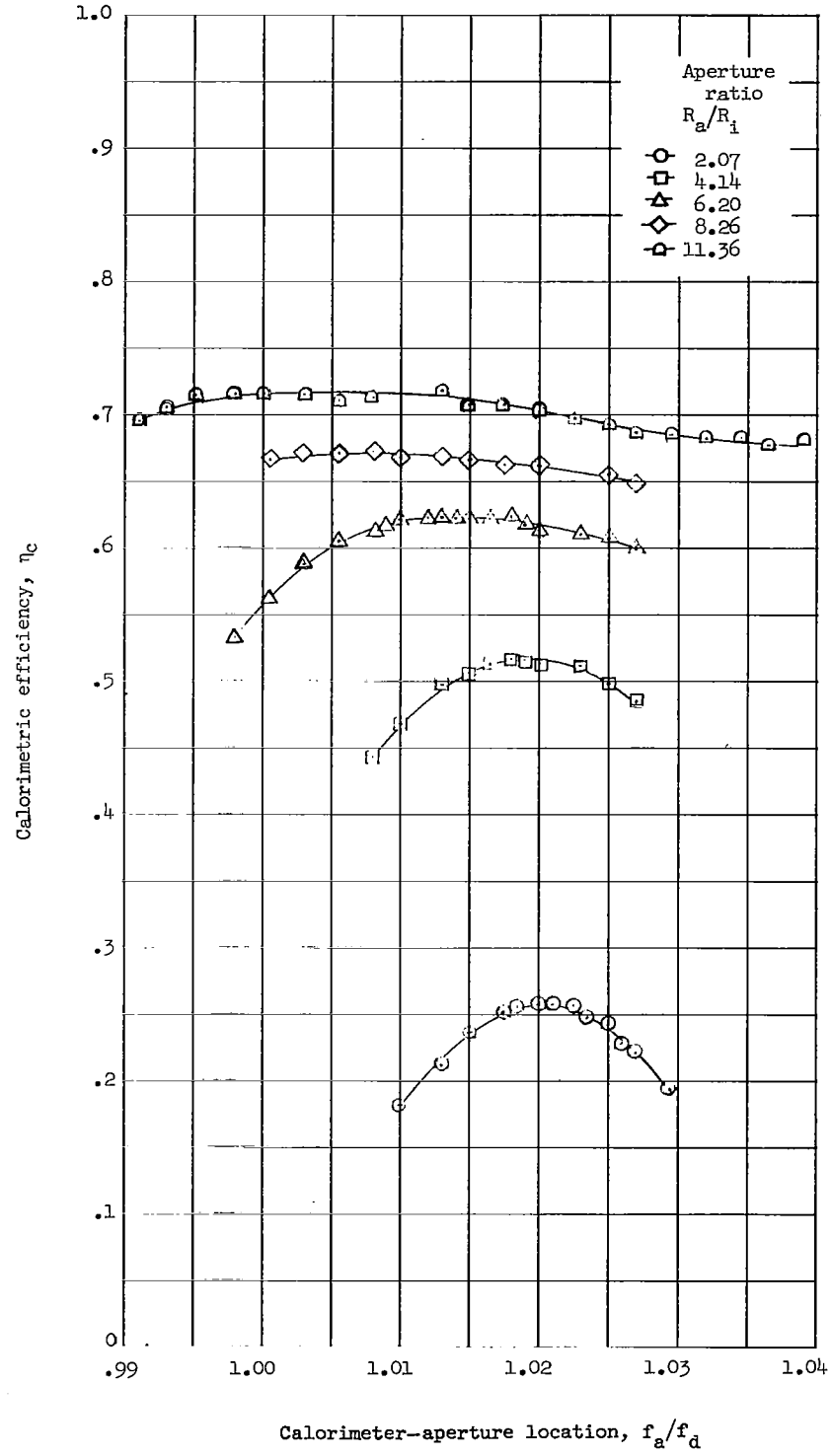

Figure 10.- Variation in calorimetric efficiency with axial location of calorimeter aperture for model 3.

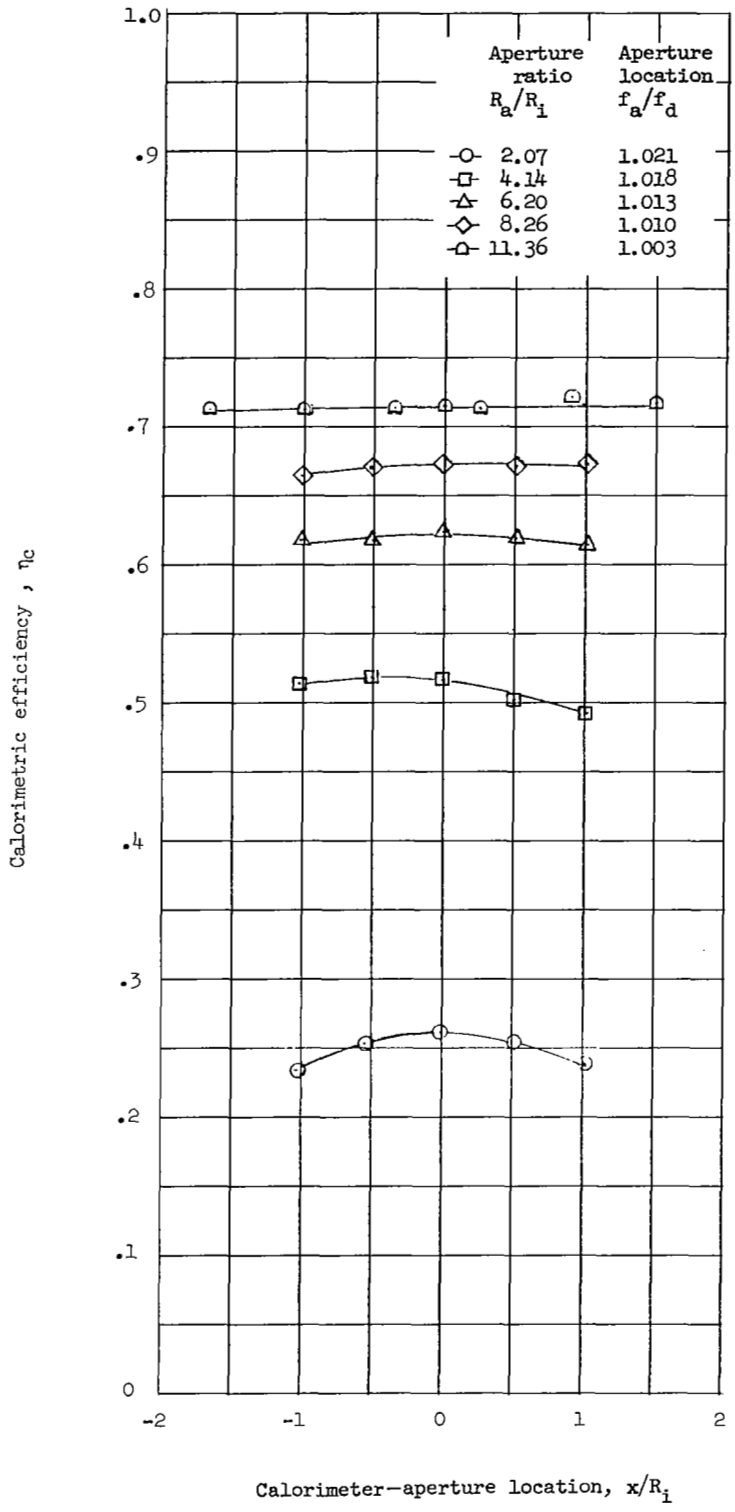

Figure 11.- Variation in calorimetric efficiency with lateral location of calorimeter aperture for model 3.

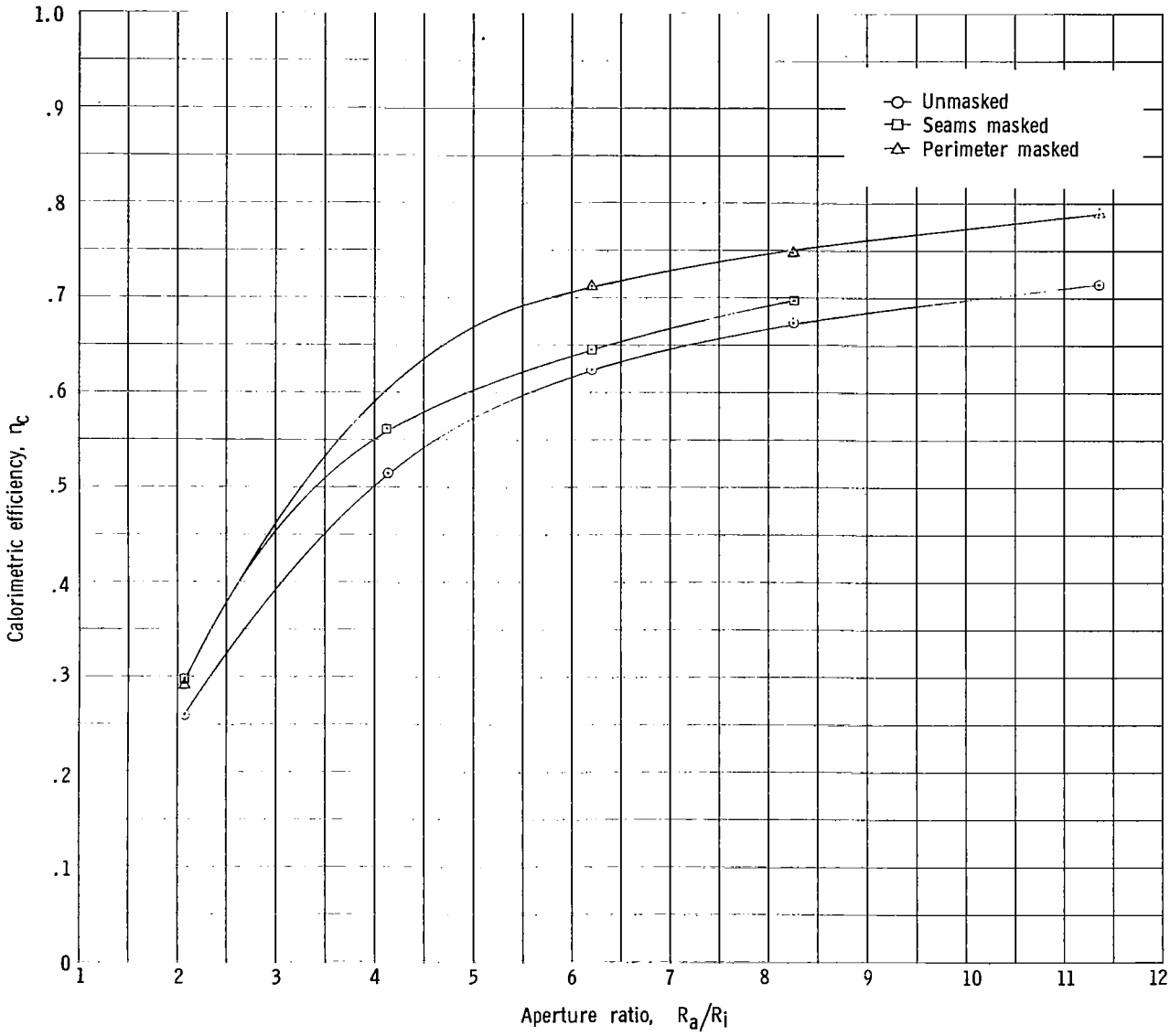

Figure 12.- Variation in calorimetric efficiency with aperture ratio for tests of model 3 in the masked and unmasked condition.

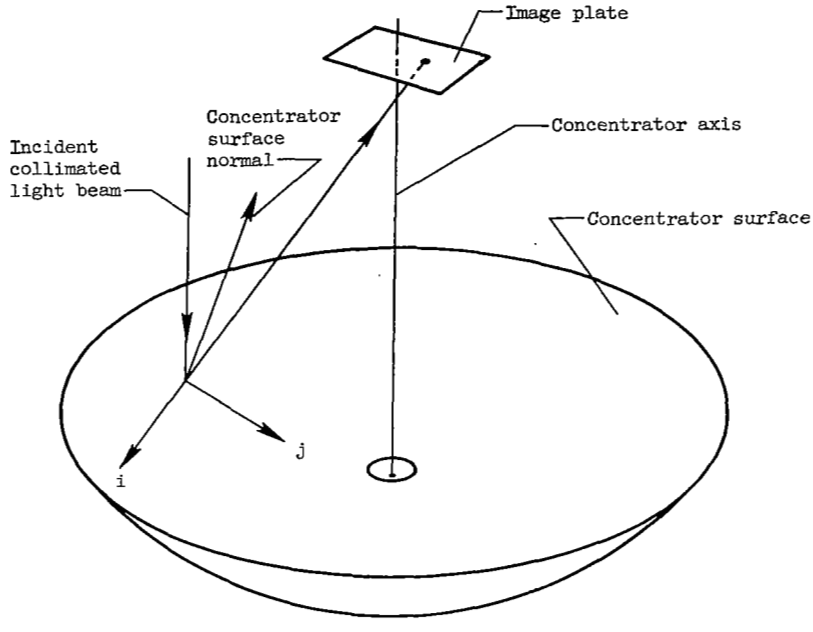

(a) Solar-concentrator ray trace.

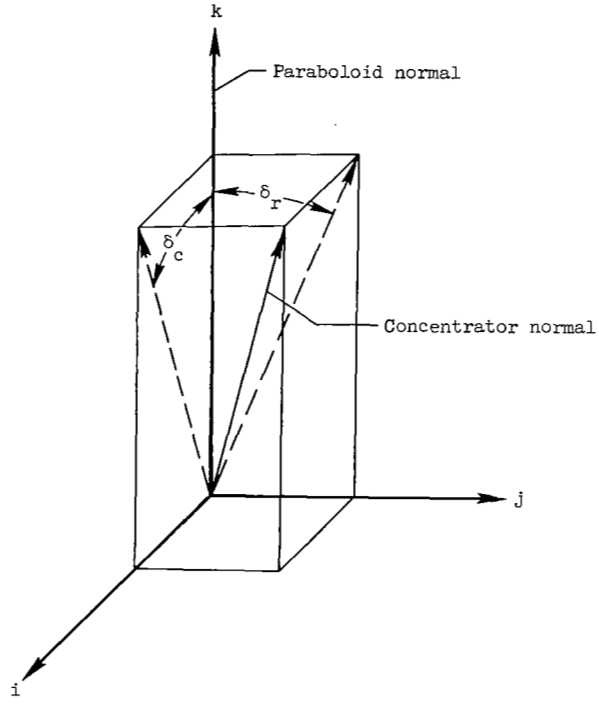

(b) Slope error.

Figure 13.- Sketch defining slope-error angles of the reflective surface.

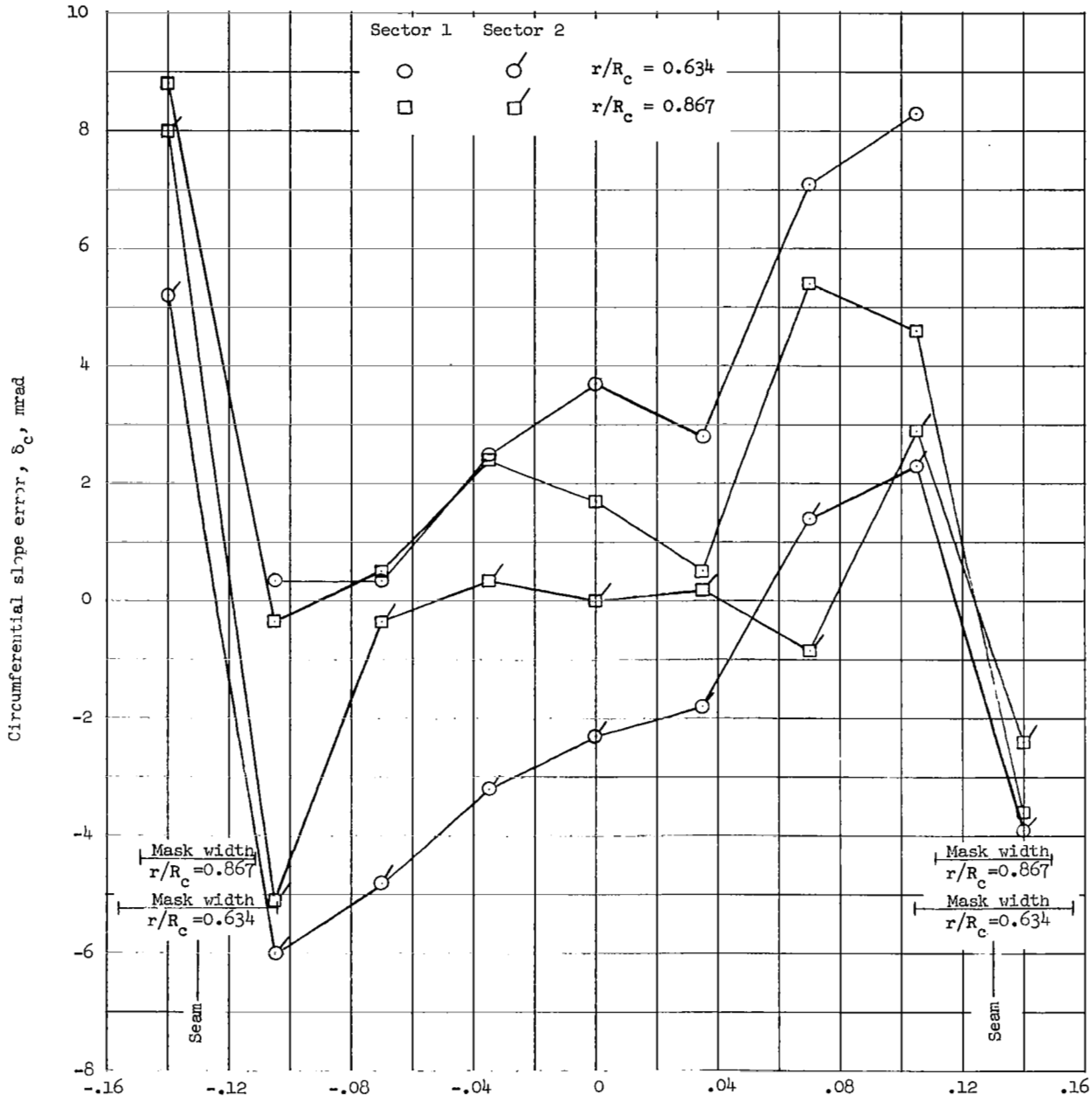

Figure 14.- Circumferential slope error across sector for model 3.

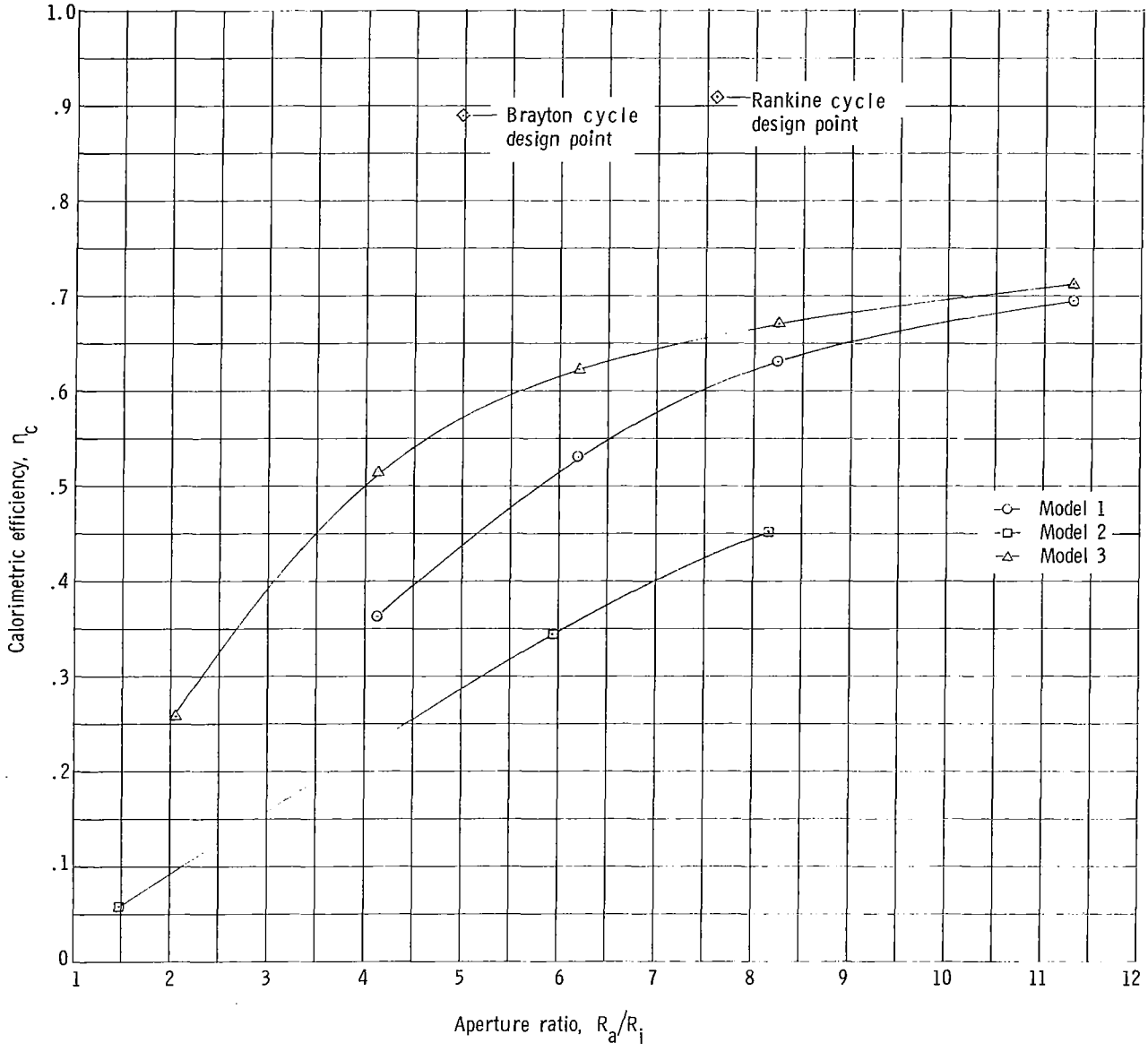

(a) Variation in calorimetric efficiency.

Figure 15.- Variation in calorimetric and geometric efficiency with aperture ratio for all three models.

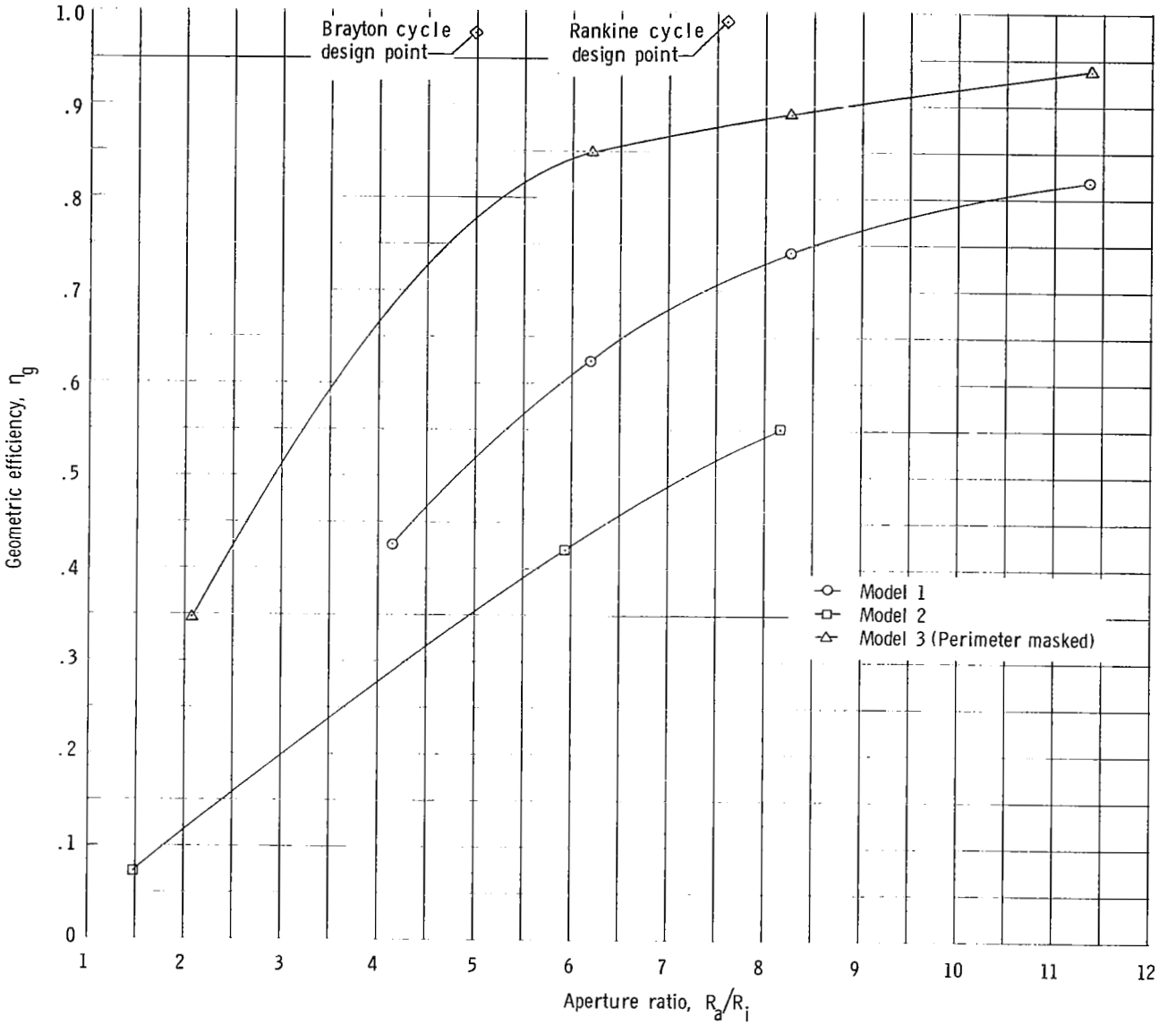

(b) Variation in geometric efficiency.

Figure 15.- Concluded.

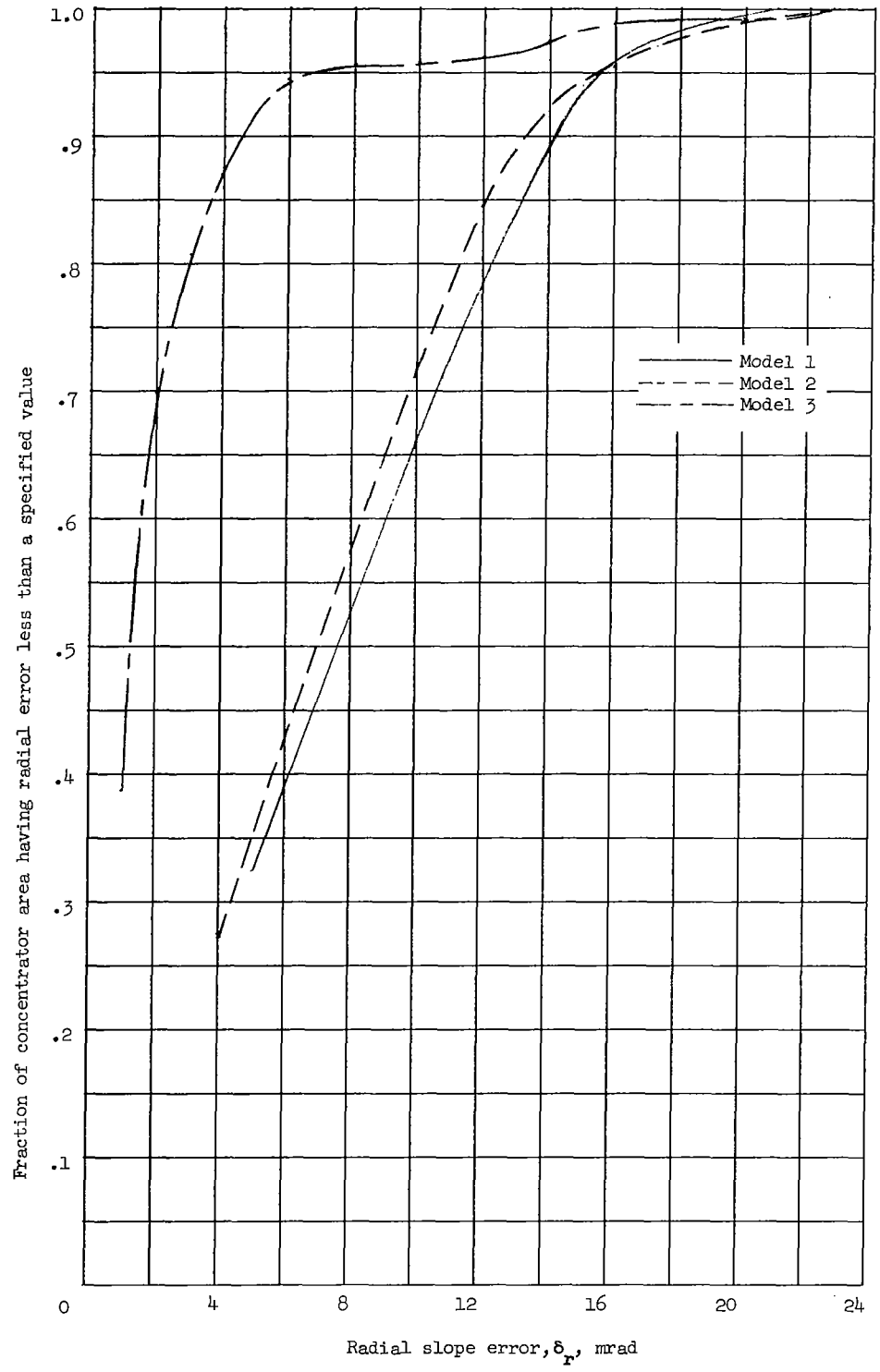

Figure 16.- Cumulative distribution of radial surface-slope error.

NASA-Langley, 1969 —— 3 L-6255

"The aeronautical and space activities of the United States shall be conducted so as to contribute . . . to the expansion of human knowledge of phenomena in the atmosphere and space. The Administration shall provide for the widest practicable and appropriate dissemination of information concerning its activities and the results thereof."

—NATIONAL AERONAUTICS AND SPACE ACT OF 1958

NASA SCIENTIFIC AND TECHNICAL PUBLICATIONS

TECHNICAL REPORTS: Scientific and technical information considered important, complete, and a lasting contribution to existing knowledge.

TECHNICAL NOTES: Information less broad in scope but nevertheless of importance as a contribution to existing knowledge.

TECHNICAL MEMORANDUMS: Information receiving limited distribution because of preliminary data, security classification, or other reasons.

CONTRACTOR REPORTS: Scientific and technical information generated under a NASA contract or grant and considered an important contribution to existing knowledge.

TECHNICAL TRANSLATIONS: Information published in a foreign language considered to merit NASA distribution in English.

SPECIAL PUBLICATIONS: Information derived from or of value to NASA activities. Publications include conference proceedings, monographs, data compilations, handbooks, sourcebooks, and special bibliographies.

TECHNOLOGY UTILIZATION PUBLICATIONS: Information on technology used by NASA that may be of particular interest in commercial and other non-aerospace applications. Publications include Tech Briefs, Technology Utilization Reports and Notes, and Technology Surveys.

Details on the availability of these publications may be obtained from:

SCIENTIFIC AND TECHNICAL INFORMATION DIVISION

NATIONAL AERONAUTICS AND SPACE ADMINISTRATION

Washington, D.C. 20546